

## Magnetic Analysis of Elastic and Reactive Scattering in Crossed Molecular Beams of K Atoms with $\text{CH}_3\text{I}$ , $\text{Br}_2$ , and $\text{ICl}$ †

R. R. HERM,\* R. GORDON, AND D. R. HERSCHBACH,

*Department of Chemistry, Harvard University,  
Cambridge, Massachusetts*

(Received 11 June 1964)

**A**NGULAR distributions of reactively scattered alkali halides have been measured in several molecular beam studies<sup>1-4</sup> of alkali atom reactions of the type  $\text{M} + \text{RX} \rightarrow \text{MX} + \text{R}$ . To distinguish the MX product from the background of elastically scattered M atoms, the detection method has relied on subtracting signals read to two surface ionization filaments: one of W or Re, which is about equally sensitive to M and MX; the other a Pt-W alloy, which under certain conditions is much more sensitive to M. Although the results obtained with this technique have usually appeared satisfactory, many materials are found to "poison" the filaments, and it is extremely difficult to obtain reproducible measurements at low scattering angles where the M background is very large.<sup>2-4</sup>

We have resorted to a magnetic deflection experiment which eliminates most of the background signal due to the paramagnetic M atoms and thus permits a direct measurement of the distribution of the diamagnetic MX molecules produced by reactive scattering. The results, shown in Fig. 1, verify for three reactions the product distributions which were derived from the two-filament method and also establish some additional features.

The beam apparatus<sup>2,4</sup> and the inhomogeneous deflecting magnet<sup>5</sup> are described elsewhere.<sup>6</sup> The beams are formed by thermal effusion (K beam at 718°K, cross beam at 310°K) from ovens mounted on a turntable which is rotated to sweep the angular distribution past the detector (K directed at  $\theta = 0^\circ$ , cross beam at  $\theta = 90^\circ$ ). For this experiment, it is essential that, with the magnet off, the profile of the signal transmitted through the collimating slits and magnet barrel to the detector should remain independent of the observation angle  $\theta$ , since broadening of the profile by misalignment or background scattering can drastically reduce the effective deflecting power. Figure 1(a) shows a typical check<sup>7</sup> of this requirement and an example of a deflection pattern. Since relatively wide slits had to be used,<sup>6</sup> about 14% of the parent K beam (including high velocity atoms and  $\sim 1\%$   $\text{K}_2$  molecules) cannot be deflected.

Measurements of the magnetically filtered signal as a function of the magnet current are illustrated in Fig. 1(b); this demonstrates that for  $\text{K} + \text{Br}_2$  a large fraction of the scattered flux at  $\theta = \pm 10^\circ$  and beyond is due to a diamagnetic product.

In Fig. 1(c) the results for reactions of K with  $\text{CH}_3\text{I}$ ,  $\text{Br}_2$ , and  $\text{ICl}$  are compared. Results obtained for the

nonreactive system  $\text{K} + \text{cyclohexane}$  are also shown; as expected, this exhibits the same transmission as the parent K beam. All of the data were obtained with a W filament (0.076 mm diam., heated with 0.55 A) except for a few points for  $\text{K} + \text{Br}_2$  (solid squares), which were obtained with a Pt-W filament (0.076 mm diam., 0.20 A) that had been "methanated" to render it insensitive to KBr and to poisoning by  $\text{Br}_2$ .<sup>4</sup> As the latter points are somewhat higher than those for cyclohexane, it appears that the Pt-W filament still detects some KBr, but with low efficiency ( $\sim 5\%$ ). The results

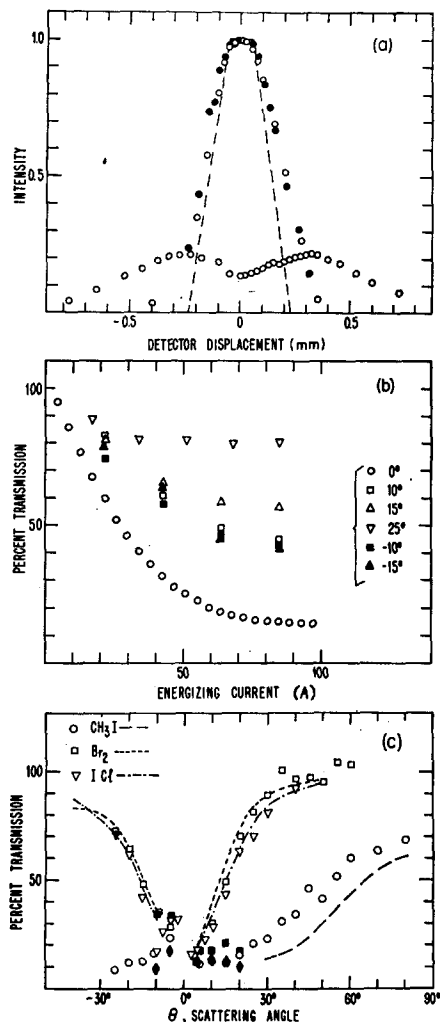


FIG. 1. Magnetic deflection analysis: (a) Beam profile (for zero field) calculated from nominal slit geometry (dashed trapezoid) compared with profiles observed for parent K beam at  $0^\circ$  (open circles; unnormalized signal  $5 \times 10^{-10}$  A) and scattered signal at  $25^\circ$  (solid circles; unnormalized signal  $5 \times 10^{-14}$  A). The Stern-Gerlach deflection pattern for the parent beam (at a magnet current of 67.6 A) is also shown. (b) Signal reaching detector (at center of beam profile) as a function of the magnet current, for scattering of  $\text{K} + \text{Br}_2$  at various angles. (c) Comparison of transmitted signal (at a magnet current of 84.4 A) versus scattering angle for beams of  $\text{CH}_3\text{I}$  (circles, long dashes),  $\text{Br}_2$  (squares, short dashes),  $\text{ICl}$  (triangles, dot-dashes), and cyclohexane (diamonds) colliding with the parent K beam. Dashed curves are results predicted from data obtained with the two-filament technique.

for the reactive systems are in very good agreement<sup>8</sup> with calculated curves (shown dashed) derived from previous two-filament measurements.<sup>2,4</sup> There is clearly a striking difference between the CH<sub>3</sub>I reaction, in which the diamagnetic product appears only at angles beyond  $\theta \approx 30^\circ$  and is accompanied by a comparable amount of elastic scattering, and the Br<sub>2</sub> and ICl reactions, in which the product is a substantial fraction of the signal within  $\theta < \pm 30^\circ$  and practically 100% of the signal beyond  $\theta \approx 30^\circ$ .

† Support received from the National Science Foundation is gratefully acknowledged.

\* National Science Foundation Predoctoral Fellow, 1961–1964.

<sup>1</sup> For reviews, see W. L. Fite and S. Datz, *Ann. Rev. Chem.* **14**, 61 (1963), and J. Ross and E. F. Greene, Report of the Solvay Congress (1962).

<sup>2</sup> D. R. Herschbach, G. H. Kwei, and J. A. Norris, *J. Chem. Phys.* **34**, 1842 (1961); D. R. Herschbach, *Discussions Faraday Soc.* **33**, 149 (1962).

<sup>3</sup> D. Beck, E. F. Greene, and J. Ross, *J. Chem. Phys.* **37**, 2895 (1962); M. Ackerman, E. F. Greene, A. L. Moursund, and J. Ross, *Intern. Symp. Combust.*, **9**, 669 (1963).

<sup>4</sup> K. R. Wilson, G. H. Kwei, J. A. Norris, R. R. Herm, J. H. Birely, and D. R. Herschbach, *J. Chem. Phys.* **41**, 1154 (1964).

<sup>5</sup> R. R. Herm and D. R. Herschbach, UCRL Report 10526 (University of California Radiation Laboratory, Berkeley, October, 1962).

<sup>6</sup> The magnet and detector assembly were mounted on a common flange and viewed the scattering center through two slits, each 0.1-mm wide; the first slit was 0.5 cm ahead of the magnet and 11.6 cm from the detector; the second slit was 6.35 cm ahead of the first and 1.4 cm from the scattering center. The magnet barrel is 7.0 cm long and the maximum width of the air gap is 0.32 cm. At an energizing current of 84.4 A, the induction in the air gap is  $B \approx 11$  kG and the transverse gradient is  $\partial B/\partial z \approx 34$  kG/cm.

<sup>7</sup> A conspicuous deviation occurs near  $\theta \approx -5^\circ$ , where the profile is much broadened by an apparatus "ghost," evidently due to reflected K atoms.

<sup>8</sup> One reason the dashed curve for CH<sub>3</sub>I is somewhat low is neglect of a correction to the deflecting power. The calculations assumed 14% K transmission at all  $\theta$ , whereas kinematics requires the laboratory velocity of elastically scattered K to increase with  $\theta$ . A rough correction accounts for about half of the discrepancy. The effect is negligible for Br<sub>2</sub> and ICl.

### Third Virial Coefficient and Intermolecular Forces for the Simple Gases

AHLBORN WHEELER

261 East Alegria Street, Sierra Madre, California

(Received 17 June 1964)

THE purpose of this note is to deduce the correct temperature dependence for the third virial coefficient of the simple gases and to point out that neither the Lennard-Jones 6–12 potential<sup>1</sup> nor 6–9 potential<sup>2</sup> reproduce this. A square-well (so-called "box") potential<sup>3</sup> gives qualitative agreement, and we suggest that a Lennard-Jones 6–15 potential might fit quantitatively.

The usual third virial coefficient  $C$  calculated for these three potentials,<sup>1–3</sup> when plotted against temperature, all give curves of about the same shape, and

inaccuracies in determining experimental values make any choice difficult. However, when the quantity  $RT$  times  $C$  is plotted against temperature, marked differences appear between the theoretical curves. We call this quantity  $C_T$ , and define it as the coefficient of  $d^2$  in the expansion of  $pV$  as a power series in the density  $d$ . We find that theory predicts two possible shapes for  $C_T$  vs  $T$ :

*Type 1:* The Lennard-Jones 6–9 and 6–12 potentials give plots of  $C_T$  vs temperature which rise uniformly from below the critical temperature,  $T_c$ , to higher temperatures, with no maximum or minimum. The 6–12 potential seems to have a point of inflection at about 1.35  $T_c$ . We locate  $T_c$  by the assumption that  $\epsilon_0/kT_c$  is about 0.8 where  $\epsilon_0$  is the depth of the potential minimum.

*Type 2:* The square-well or box potential gives curves which rise to a maximum located slightly below  $T_c$ , then descend through a point of inflection to a minimum at about 1.5  $T_c$  and then rise uniformly again at higher temperatures. The exact position of the maximum and minimum depend on the width of the box.

To decide whether real gases obey Type 1 or Type 2 curves, we have considered in detail the very accurate experimental data of Michels<sup>4</sup> and of Beattie<sup>5</sup> on argon and xenon. As expected, the actual experimental values of  $C_T$  calculated by Michels and Beattie are not smooth enough to make a decision, except between  $T_c$  and about 1.5  $T_c$  the values for xenon are decreasing markedly for both experiments. This already suggests that Type 2 is followed.

We next make the key move of examining the very accurate data on the internal entropy  $S_i$  and on the heat capacity at constant volume,  $C_v$ , which Michels has computed from his data. The first derivative of  $C_T$  with respect to temperature is directly proportional to the curvature at low densities of a plot of  $-S_i$  vs  $d$ , while the second derivative<sup>6</sup> of  $C_T$  with respect to temperature is proportional to the low-density curvature of a plot of  $-C_v$  vs  $d$ . Type 2 behavior demands that the curvature of  $-S_i$  vs  $d$  should be zero at about 1.5  $T_c$  and should be negative below this temperature and positive above this temperature. On examining Michels' entropy data for argon and xenon, we find exactly this. At  $-50^\circ\text{C}$  for argon (which is 1.48  $T_c$ ) we find zero curvature, while at lower temperatures the curvature is distinctly negative and at higher temperatures, distinctly positive. The xenon entropy data shows a similar result, although they do not extend high enough in temperature to display positive curvature, which all theories demand in any case.

Since Type 2 behavior demands a point of inflection just above the critical temperature (in the  $C_T$  vs  $T$  plot), we next examine the curvature of plots of the heat capacity  $-C_v$  vs  $d$ . For both argon and xenon these plots have distinctly negative curvature (at low density) below  $T_c$ , zero curvature at about 1.1  $T_c$